PAPER

Non-toxic luminescent Au Nanoclusters@Montmorillonite nanocomposites powders for latent fingerprint development†

Yanlin Yu, [ID] [ab] Lei Yan [ID] *[a] and Zhining Xia[b]

Non-toxic Au nanoclusters@montmorillonite (AuNCs@MMT) nanocomposites with strong red fluorescence are prepared by a microwave (MW)-assisted synthesis method and immobilize Au NCs into sodium MMT clay matrix *via* electrostatic interaction. Due to the immobilization of Au NCs in the layered structure of the MMT clay matrix, the formative AuNCs@MMT nanocomposites show high emission, stable chemical features and less toxicity. The obtained Au NCs and AuNCs@MMT nanopowders were characterized by using UV-visible absorption spectroscopy, fluorescence spectroscopy, infrared spectroscopy, TEM/HRTEM, SEM and XRD *etc.* to depict their sizes, microstructures and optical features. Due to their environmentally friendly preparation, time-saving procedure, user-friendly operation, low cost, efficient UV-visible radiation-dependent photoluminescence and good affinity with finger residues, the as-synthesized AuNCs@MMT nanopowders are employed as a alternative florescent developing reagent for enhancing latent fingerprints deposited on various object surfaces (such as glass, porcelain enamel, stainless steel, painted metal, plastic products, weighing papers *etc.*) for individual identification. As results, the enhanced fingerprints with clear patterns and satisfactory ridge details were obtained by using as-prepared AuNCs@MMT nanopowders. At the same time, intensively red fluorescence as well as good contrast without background staining of developed prints demonstrated great advantages for surfaces with multicolour. Because of their good sensitivity, non-toxicity and strong resistance to background interference, the as-prepared fluorescent nanocomposites are an actual alternative to conventional powdering reagents, which may find potential application in forensic detection.

Introduction

Due to their good magnetic properties, unique size-dependent photoluminescence with stable emission, high quantum yield and good biocompatibility, nanomaterials, such as magnetic nanoparticles, semiconductor quantum dots and their composites, metals and their oxide nanoclusters, as well as carbon dots, are highly attractive for latent fingerprint visualization.[1–10] Among them, gold nanomaterials, for instance, colloidal gold, gold nanocomposites, gold nanopowders and gold nanoclusters (Au NCs), have been employed to enhance fingerprints from the late 80 s of the last century.[11–20] Originally reported in 1989, Saunders *et al.* first tested and verified the possibility of employing gold nanomaterials for latent finger-marks development, and multi-metal deposition (MMD) has been proposed at the same time.[11] Two metals, silver and gold

were employed to enhance latent fingermarks. In order to improve sensitivity of the method, enhance contrast and observe micro morphology of developed prints, relative researches have been performed and good results were obtained. Schnetz and Margot investigated the power of MMD method, and optimized conditions of particulate size, pH, reagent, handling were obtained.[12] In Choi's report, scanning electron microscopy (SEM) has been firstly used to investigate the binding of gold nanoparticles to fingermarks deposited on nonporous surfaces.[13] The results demonstrated that gold nanoparticles, formed by standard MMD procedure, bind preferentially to ridges on nonporous surfaces. Despite the MMD method is sensitive to aged fingermarks and valid for variety object surfaces, sophisticated reagents, time-consuming procedures and strict pH ranges limited the application. Based on this method, single-metal deposition (SMD) method has been proposed by Stauffer and his co-workers.[14] In the processing of SMD, the silver enhancement of the gold colloids was replaced by a gold enhancement procedure and only one metal (colloidal gold) was used. Comparing with MMD process, SMD method shows simplified operation, reduced cost and increased efficiency. Thereafter, several groups reported the use of gold nanomaterials for latent finger-marks detection and

[a]School of Criminal Investigation, Southwest University of Political Science and Law, Forensic Science Engineering Research Center of Universities in Chongqing, Chongqing 401120, China. E-mail: yanlei@swupl.edu.cn

[b]School of Bioengineering, Chongqing University, Chongqing 400044, China

† Electronic supplementary information (ESI) available. See DOI: 10.1039/c7ra09444b

enhancement. For instance, a simple and environment friendly chemical route for developing latent fingermarks by one-step gold nanoparticles deposition method was reported by Gao *et al.* and the developed prints provided sharp and clear ridge details, without background staining.[15] Based Au NCs with strong fluorescence and good biocompatibility, Leggett and his co-workers determined a novel method of fingerprinting, which could detect ridge patterns and simultaneous estimate the person who deposited the fingermarks is a smoker or not.[16] Since then, researchers focus on developing new reagents and novel approaches for enhancement of latent fingerprints while analysis of fingerprints residues, such as explosive and drugs.[3,17,18] Moreover, by *in situ* growth of gold nanoparticles on ridge patterns, Hussain's group developed a single step approach to make latent fingerprints visible and visualizing latent fingerprints by electrodeposition of gold nanoparticles were also reported.[19,20] However, most of these developing studies were carried out in a narrow pH range or by using aqueous solution of gold nanomaterials as developing reagents, which might bring some irreversible damages to the objects with porous surfaces. In addition, some of the studies were time-consuming and not user-friendly. Hence, powder technique possess characteristics of facile operation, nondestructive for fingerprint residues and objects surfaces is still a noteworthy method for visualizing latent fingerprints and research will be focused on preparing novel powders with unique features.

Montmorillonite (MMT) is a very soft phyllosilicate group of minerals. Low-cost, environmentally friendly and its porous characteristics make it attract more and more attentions. And it was used as a matrix material to form kinds of complex substances with different properties. CdTe–montmorillonite nanocomposites were synthesized by *in situ* intercalation of CdTe quantum dots (QDs) into a sodium montmorillonite clay.[21] The products with different emissions were used as developing powder enhanced latent fingermarks, and the developed prints were well-defined in the terms of ridge details. However, the third-level of ridge characteristics (sweat pores) were not presented in their images. In addition, CdTe QDs are known as a highly poisonous material, the toxicity of the powder cannot be ignored, which will increase the risk of harm to the operators.

Here, we demonstrate for the first time that AuNCs@MMT nanocomposites can be prepared *via* electrostatic interaction and the resulting powders show strong red fluorescence under UV-visible light irradiation. The procedure is emerging as a rapid, effective and environmentally friendly method for preparing fluorescent nanocomposites. The main attribute of this work is that our red emitting AuNCs@MMT nanocomposites could be conveniently synthesized in a few minutes without complicated experimental processing and conditions as well as toxic chemicals and solvents. The synthetic conditions including the applied MW programme and the concentrations of Au NCs are reported. The Au NCs and AuNCs@MMT nanocomposites are well characterized by various spectroscopic techniques and electron microscopes. Finally, the potential use of AuNCs@MMT nanocomposites for developing latent fingermarks is explored. The obtained fluorescent powders of AuNCs@MMT nanocomposites may find potential application in forensic science for individual identification.

Experimental

Chemicals

Sodium hydroxide (NaOH), hydrochloric acid (HCl) and hydrogen nitrate (HNO$_3$) were purchased from Chongqing Chuandong Chemical (Group) Co., Ltd. (Chongqing, China). Na$^+$-montmorillonite (Na$^+$-MMT, purity > 98%) was purchased from NANOCOR company (CEC is 145 (meq/100 g) $\pm$ 10%). Hydrogen tetrachloroaurate$_{\text{III}}$ trihydrate (HAuCl$_4$·3H$_2$O) was obtained from Aldrich (Milwaukee, WI, USA). Bovine serum albumin was purchased from Sigma-Aldrich (St. Louis., MO, USA).

All chemicals of analytical reagent grade were used without further purification. Ultrapure Millipore water (18.2 Ω) was used throughout all the experiments.

Preparation of the Au NCs and Au NCs@MMT nanocomposites

According to our previous reports, Au NCs have been obtained by a one-pot microwave (MW)-assisted hydro-thermal method with some modifications.[22] All glassware was washed with aqua regia. In a typical experiment, 1.0 mL of 65 mg mL^{-1} BSA solution was added to 1.0 mL of 10 mmol L^{-1} HAuCl$_4$ solution, followed by 0.10 mL of 1.0 mol L^{-1} NaOH solution. The mixed solution was then transferred to a teflon high-pressure digestion tank and heated by MW programme radiation (800 W) for 30 s and the reaction mixture turned to dark brown.

In a typical adsorption experiment, 2.0 mL as-synthesized Au NCs solution was added into 0.2500 g Na$^+$-MMT powder. After ten minutes-magnetic stirring, the precipitate were separated by centrifugation and dried at 35 °C under vacuum condition. The products displayed an intensive red fluorescence emission under UV light (365 nm), indicating the formation of AuNCs@MMT nanocomposites. The as-prepared Au NCs solution and AuNCs@MMT powders were characterized by UV-visible absorption spectroscopy, fluorescence spectroscopy, infrared spectroscopy (IR), X-ray photoelectron spectroscopy (XPS), scanning electron microscope (SEM), transmission electron microscope/high-resolution transmission electron microscope (TEM/HRTEM) and X-ray diffraction (XRD).

Apparatus

Fluorescence measurements and quantum yield were performed on an Rf-5301PC fluorescence spectrometers (Shimadzu, Japan) and an FLS980 series of fluorescence spectrometers (Edinburgh instruments, UK), respectively. An UV2450 UV-visible absorption spectrophotometer (Shimadzu, Japan) and an U4100 UV Spectrometer (Hitachi, Japan) were used to measure absorption spectra of Au NCs solution and Au NCs@MMT powders, respectively. XRD patterns were performed on a D8 ADVANCE X-ray diffractometer (Bruker, Germany) with the following parameters: Cu Kα, 40 kW at 30 mA,

step size is 0.02°, scan angle range is 10–80°. XPS was conducted on an ESCALAB 250XI photoelectron spectrometer (Thermo-Fisher Science, USA). Infrared spectra were performed on an IR Prestige-21 Fourier transform infrared spectrophotometer (Shimadzu, Japan). All spectra were taken at 25 °C. The micro-structures of as-prepared nanomaterials were characterized by a Tecnai F-20 field-emission HRTEM (FEI Corporation, USA) operating at 200 kV and an S4800 field emission scanning electron microscope (Hitachi, Japan). The average particle size and zeta potential of the product was measured by a Zetasizer Nano ZS90 (Malvern, UK). A D8023CSL-K4 domestic microwave oven (Galanz, China) was used to synthesize Au NCs. An HJ-3 magnetic stirrer (Jintan Xinhang Instrument Factory, China), a mini centrifuge (ExtraGene Instrument Company, USA, 6000 RPM) and a DZF-6050 vacuum drying oven (Shanghai Jing Hong Laboratory Instrument Co., Ltd., China) were employed for preparing, separation and drying. In the procedure of taking photographs for developing powder, a ZF-5 Handheld UV analyzer was employed to provide light source and photos were recorded by using a Nikon digital camera D7000 with a micro-lens of AF-S Micro NIKKOR 40 mm 1: 2.8G. A VSC5000 document imaging workstation (Foster & Freeman Ltd., UK) and a VHX-S550E digital microscope (KEYENCE CORPORATION, Japan) were also used to observe and take pictures of developed prints.

Detection of latent fingerprints

All sebaceous latent fingermarks were obtained from a volunteer by gently rubbing fingertips against the forehead and stamping them onto various surfaces at the same condition. Glass slides, painted metal, plastic products, stainless steel and porcelain enamel were chosen as non-porous substrates for depositing latent fingerprints. Weighing paper was used as porous substrates. And a multi-coloured ceramic mug with sophisticated patterns was also employed for experiments. Commonly used powder techniques were carried out in all visualization procedures. And the processing could accomplish in one hour.

Results and discussion

Synthesis and characterization of Au NCs and Au NCs@MMT

Au NCs with different chemical components (e.g., Au_3, Au_8, Au_{10}, Au_{13}, Au_{25}, etc.) have been successfully prepared by "bottom-up" and "top-down" strategies.[23–27] These Au NCs with different sizes possess different photoluminescence features (such as excitation and emission wavelength as well as quantum yield), some of them emit blue fluorescence, some of them own green or red emission, etc. All of these Au NCs can be used as fluorescence probes. In this experiment, Au NCs with red fluorescence were selected to compose developing powder, due to its strong emission, good sensitivity for the human eyes, wide range of excitation wavelength and most importantly, good ability to resist background fluorescence interference.

Au NCs with intensively red photoluminescence were synthesized by using microwave irradiation method. By the environment-friendly and high-efficiency method, a dark brown solution of Au NCs was prepared which would be employed as a fluorescent probe to prepare developing reagent for latent fingerprints detections. In our previous studies, it was found that excessive heat from the MW irradiation would reduce quantum yield of fluorescent AuNCs.[22] Consequently, a MW programme consisting of 15 seconds MW irradiation, 30 seconds pause, and 15 seconds MW irradiation was applied to subsequent MW-assisted preparation of fluorescent Au NCs. Compared with our previous methods, a teflon high-pressure digestion tank is employed as the reaction vessel to replace beaker in this study, which is beneficial to form high temperature and pressure in such a short span of tens seconds. Hence, the reaction time can be shortened from several minutes to a few seconds, thanks to the super-heating and high pressure. The reaction mixture turns from light yellow to dark brown after MW irradiation (inset of Fig. S1a†) which is consistent with our previous work.[22] Similarly, the solution of products emit an intense red fluorescence (inset of Fig. S1a†) under UV light ($\lambda = 365$ nm) as well as green light. The formation of these fluorescent particles is attributed to the in situ reduction of Au^{3+} to Au^0 embedded in the BSA molecules. Subsequently, the aggregated Au atoms form minor sized Au NCs of highly fluorescent.[28] And a broad emission band (550–750 nm) with an emission peak maximum of 640 nm is observed. The maximum excitation wavelength is 525 nm, which is green light. Compare to UV light, green light owns lower energy, can excite less substrates, which also means it could reduce background interferences. Furthermore, take green light as an alternatives of UV light will decrease the health risk of examiners. Fig. S1b† displays the UV-visible absorption spectrum of reactants and the Au NCs product. An absorption peak of 530 nm demonstrates the formation of Au NPs, which do not appear in the spectra of BSA and $HAuCl_4$.

Solid form of the as-synthesized Au NCs was obtained by adjusting pH value of solution from alkalinity to acidity.[22] After vacuum drying, the powders of Au NCs also possess very strong red emission under UV light and green light irradiation. As we know, main constitute of the nanopowders is BSA, which is easily to form crystalline solid. Therefore, the dispersion degree and grain size of as-synthesized Au NCs powder is not very satisfactory for latent fingerprint detection. In order to improve the property of gold nanopowders, Na^+-MMT powder, a natural clay with porous structure, was chosen as the matrix for immobilization Au NCs. The procedure of preparation AuNCs@MMT nanocomposites is depended on electrostatic interaction between negatively charged Au NCs and positively charged sodium ion, which are dispersed in aqueous solution and modified into the inner surfaces of MMT clay, respectively. In order to confirm above-mentioned deduction, zeta potential of the as-prepared Au NCs was measured. The zeta potential of Au NCs solution was determined to be −28.4 mV at pH 10, demonstrating that the Au NCs can be easily attracted to positively charged sodium ions by electrostatic interaction. At the same time, it also indicates that the Au NCs solution has good stability which is beneficial for its storage, preservation and application. Consequently, the same as Au NCs, as-prepared

powders of AuNCs@MMT nanocomposites emit an intense fluorescence under UV light ($\lambda = 365$ nm) and green light.

Besides the size of Au NCs, its proportion in the AuNCs@MMT product is the other main factor on the performance of latent fingerprint staining. The higher load amount of AuNCs immobilized into MMT, would produce better sensitivity and resolution. In this experiment, ten minutes-magnetic stirring was used to assist the electrostatic adsorption process, and we found that the color of Au NCs solution got lighter and no longer changes, which means the adsorption of Au NCs on MMT has been saturated.

Fig. 1a depicts the fluorescence excitation and emission spectra of AuNCs@MMT nanocomposites powders prepared under optimized conditions. Compared with no fluorescent clay powders, as-prepared AuNCs@MMT nanocomposites powders owns strong red emission (Fig. 1a and inset of Fig. 1b). In the range of 600–700 nm, a finger-like emission spectrum with an emission peak maximum of 655 nm is observed. The maximum excitation wavelength (λ_{ex}) is at 525 nm which is in agreement with the solution of Au NCs and was selected for the subsequent fluorescence measurements. In summary, these results demonstrate that fluorescent Au NCs endue MMT clay the red emission, makes the AuNCs@MMT nanocomposites could be supposed as a fluorescent probe for fingerprinting. And quantum yield of the as-prepared AuNCs@MMT nanocomposites powders were measured to be 1.16%. Although this data is below the value of Au NCs solution, strikingly red fluorescence still cause enough contrast for the detection of latent fingermarks. Fig. 1b depicts absorption spectra of bare MMT clay powders and AuNCs@MMT nanocomposites powders. No significant absorption peaks and changes were detected, which means small amount of Au NCs that is immobilized to the MMT clay does not change the UV absorption characteristics of the MMT clay. The inset of Fig. 1b shows the photographic images of AuNCs@MMT nanocomposites taken under broad sunlight and UV light ($\lambda = 365$ nm). As can be seen, the powders of Au NCs@MMT nanocomposites own good dispersion and emit an intense red fluorescence under UV light (365 nm).

The morphology of BSA–Au NCs bioconjugates, bare MMT clay powder and as-prepared AuNCs@MMT nanocomposites were studied by using TEM/HRTEM and SEM. Fig. S2† displays the HRTEM and TEM images of BSA–Au NCs bioconjugates. The TEM and HRTEM images indicate that the average diameter of

Au NCs is *ca.* 4 nm and NCs are well-dispersed, which is consistent with the particle size test results (the average diameter is 4.085 nm). The lattice fringes of the Au NCs are consistent with metallic Au having a discerned lattice spacing of 2.3 Å, corresponding to the *d* spacing of the {111} crystal plane of Au, which is consistent with the literature.[29] The selected area electron diffraction (SAED) pattern also indicates that the well organized Au nanocrystals are formed in the Au NCs. SEM image of bare MMT clay powders indicates that micron-sized near-spherical particles with lamellate structure provide more surfaces for immobilization of Au NCs. The layered structure is beneficial to increase the loaded amount of Au NCs, which is also means the fluorescent intensity of AuNCs@MMT powders would be improved. Consequently, high sensitivity of latent fingerprints detection could be obtained. Furthermore, compare to micron-sized MMT clay powder, nano-sized Au NCs almost invisible, so there is no obvious image of Au NCs been observed from SEM images (Fig. 2). At the same time, due to extremely low relative content, no signal of gold was determined in the EDX measurement.

In order to obtain additional information regarding the AuNCs@MMT nanocomposites, XPS, XRD and IR of the as-prepared powders were conducted and the results are displayed in Fig. 3. The binding energy (BE) of the Au 4f$_{5/2}$ and Au 4f$_{7/2}$ peaks is 84.0 and 87.7 eV (Fig. 3a and b), respectively, and the ΔBE is 3.7 eV, inferring that elemental Au NCs are entrapped in the layered structure of MMT clay. The phase structure of bare MMT clay and the AuNCs@MMT fluorescent nanocomposites were characterized by XRD measurements. The corresponding XRD patterns, shown in Fig. 3c displays exactly the same spectra, which indicates immobilization of Au NCs will not change the phase structure of MMT clay powders. Furthermore, Fig. 3d depicts the IR spectra of bare MMT clay (bottom), BSA (middle) and the as-prepared AuNCs@MMT nanocomposites (top). From our previous study, we know that the formation of Au NCs bring little changes for the IR spectrum of BSA, inferring that the Au NCs embedded in BSA would not affect the surface-structure of BSA.[22] Nevertheless, compare with IR spectrum of bare MMT clay, distinct changes were observed in the IR spectrum of AuNCs@MMT nanocomposites. More details of infrared characteristic bands and absorption peaks were obtained, which are come from BSA. The results confirm
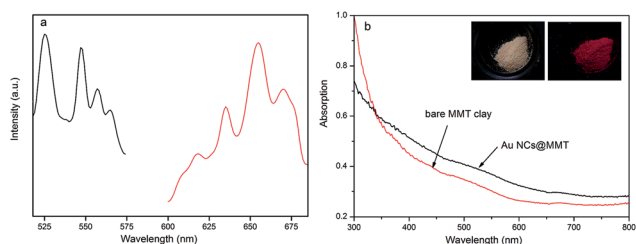

Fig. 1 (a) Fluorescent spectra and (b) absorption spectra of bare MMT clay powder and Au NCs@MMT nanocomposites powder, inset: photographic images of Au NCs@MMT nanocomposites powder taken under broad sunlight (left) and UV light ($\lambda = 365$ nm) (right).
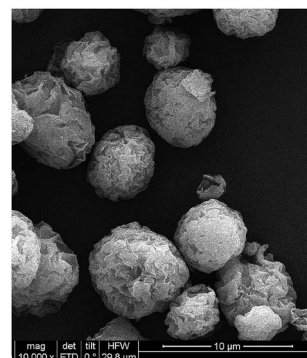

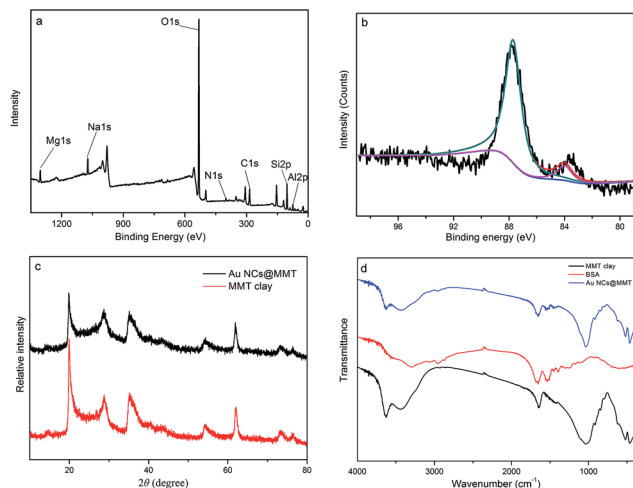**Fig. 2** SEM image of as-prepared Au NCs@MMT nanocomposites.

Fig. 3 XPS spectra of (a) survey scan and (b) Au 4f for Au NCs@MMT nanocomposites. The solid lines are obtained from the instrument curve fitting program. (c) XRD patterns of bare MMT clay powders (bottom) and the as-prepared Au NCs@MMT nanocomposites powders (top). (d) Infrared spectra of bare MMT clay powder (bottom), BSA (middle) and the as-prepared Au NCs@MMT nanocomposites powder (top).

the presence of BSA-stabilized Au NCs, which also means fluorescent Au NCs are successfully embedded in MMT clay.

Application to latent fingermarks detection

To obtain obviously contrast against the surface on which the fingerprints are deposited is the premise for choosing developing reagents. Fluorescent powders can help us to reduce background interference and improve sensitivity and contrast. Fig. 4 displays the photographs of latent fingerprints visualized
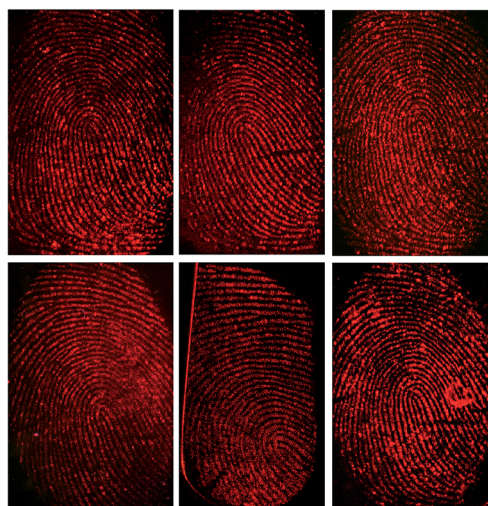

Fig. 4 Latent fingerprints on various object surfaces developed with the as-prepared Au NCs@MMT nanocomposites powders. From left to right: weighing paper, binder clips, slide glass, transparent adhesive tape, tweezers and porcelain enamel. Images were taken under UV light ($\lambda = 365$ nm).

by using as-prepared AuNCs@MMT nanocomposites powders as a fluorescent developing reagent on various object surfaces. After using the conventional powder technique, high-quality prints with strong red fluorescence were obtained under the UV light, and little background staining was observed. No matter on the non-porous or porous surfaces, the developed prints showed clear patterns and good contrast. On these smooth, polished surfaces, such as slide glass and stainless steel (tweezers), ridge details were easily recognizable. Furthermore, minutiae of ridges can be marked for individual identification. The little background staining in the image of treated print on porcelain enamel was caused by uneven surface. Latent fingerprints left on the painted metal (binder clips) and plastic surfaces (the smooth side of transparent adhesive tape) were also detected by the AuNCs@MMT nanocomposites powders. Cambered surface of binder clips caused a little difficulty for photograph, in addition, a very few air bubbles and fluorescent fibers stacked to the sticky surface of transparent adhesive tape brought a little barrier for the observation of ridge characteristics. Again, the treated prints still showed distinct ridges. In order to investigate the developing ability for porous surface, AuNCs@MMT nanocomposites powders were employed for enhancement of latent fingerprints deposited on weighing paper. Although the background interference from fluorescent ingredients of paper reduced contrast, patterns of fingerprints also can be obtained.

Multi-coloured surfaces often own sophisticated patterns and different shades. It is difficult to obtain clear ridges and good contrast for latent fingerprints on theses surfaces by using only one kind of conventional powders, no matter dark powders or light powders. In order to solve this problem, fluorescent powders based on some kind of pigments or dyes have been employed as ingredients of developing reagents. At the same time, UV light is usually employed as the excitation light source with the use of fluorescent reagents. Compare with visible lights, UV light possess higher energy as we know it, which also can excite background fluorescent materials. If both developing powder and background materials have the same or approximate fluorescent emitted wavelengths, it is not easy to distinguish developed prints. As-prepared AuNCs@MMT nanocomposite is a newly-developed fluorescent powder which differentiates from most conventional fluorescent developing reagents, it not only can be excite by UV light but also visible light (green light).

Fig. 5 displays the images of developed fingerprints on the bottom of a ceramic mug, which were excited by sunlight and UV light ($\lambda = 365$ nm), respectively. Despite its light colour under sunlight provide an extremely weak pattern impression for backdrop it showed intensively red fluorescence under UV light (365 nm). Under sunlight condition, it is almost impossible to distinguish developed ridges from the yellow-based multicolour background. However, take UV light as an alternative excitation light source, clear ridges patterns and minutiae points with highly red fluorescence could be obtained, relatively dark background provided good contrast, hardly any interference was recorded. In order to observe more details of the ridge, a document imaging workstation was employed. As
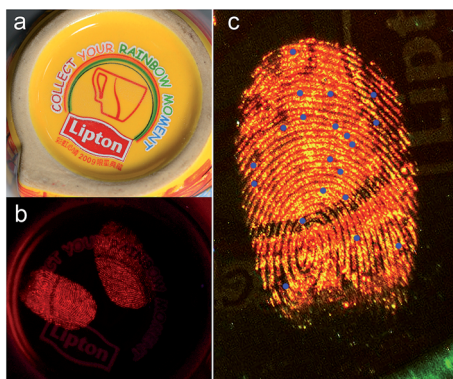
Fig. 5 Images of developed fingerprints on the bottom of a ceramic mug. Images were taken under sunlight (a) and UV irradiation (λ = 365 nm, b and c), respectively. (c) Long pass filter was used, and ridge details points are marked.
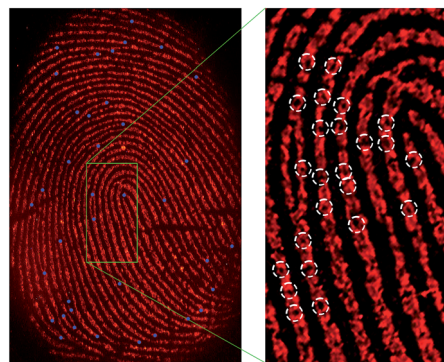

Fig. 6 Images of developed fingerprints on the plastic Blue-ray CD discs (the smooth side for burning). UV light was employed as excitation light source and a VSC5000 document imaging workstation was used to take pictures. The right image was enlarged by photoshop.

can be seen from Fig. 5c, the second-level of ridge characteristics, such as bonding point, bifurcation and ridge termination, can be recognized, those are useful in matching a fingerprint to a specific person. And the number of these second-level characteristics is more than twenty, which is enough to guarantee the accuracy of identification. Consequently, taking visible light as the excitation light source could avoid common background fluorescence interferences. As such, it should be attractive for further applications in latent fingerprints visualization. At the same time, use visible light replace UV light would avoid UV damage for the substrates and examiners. Furthermore, the visualization process is accomplished by powder technique, due to avoid contact with organic solvents and dyes, this fluorescent powder reduced the harm for the operators.

In order to evaluate its stability under normal site inspection working conditions, AuNCs@MMT nanocomposites powder was prepared and placed in an ordinary plastic box for seven months, which experienced more than 60 days of sustained high temperature over 30 °C (in July and August). Then it was been used as a developing powder for enhancement of a fresh sebaceous latent fingerprints deposited on plastic surface (Blue-Ray CD discs). As can be seen from Fig. 6, developed prints exhibits clear ridges and minutiae points, even for the third-level of ridge characteristics (sweat pores). The result suggested that the as-prepared AuNCs@MMT nanocomposites powder owns good stability, and its highly red emission cause enough contrast for latent fingerprints visualizing, which is applicable to on-site investigation works. Comparison with semiconductor quantum dots in resolution, the as-prepared AuNCs@MMT nanocomposites powder owns considerable developing ability (such as in resolution, sensitivity and contrast), or better. Moreover, the powder technique is easier to preserve and operate than the solution method.

The right image of Fig. 6 presents the well-defined boundary between ridge and valley areas of the fingerprint. By comparing magnified images of ridge detail with valley regions, we can confirm directly that the majority of AuNCs@MMT nanocomposites powder bind to the ridges with little amounts bound to valley areas. The results indicated that powders

adhered to the fingerprint residues. The principle is the same as the conventional powder technique, that is the electrostatic interactions between the powder and moisture or/and oily components of the fingerprint residues.[30]

In this study, no toxicity assessment of the as-prepared AuNCs@MMT nanocomposites was performed. The presumed non-toxicity of AuNCs@MMT nanocomposites was only based on studies found in the literatures.[31–35] It is shown that Au NCs exhibits no increased risk, unlike the cadmium based quantum dots and organic dyes, which could release free toxic cadmium ions and volatilize toxic organic compounds, respectively. Au NCs can be used as biocompatible probe for cellular imaging,[31,32] tumour imaging and deep tissue therapy.[33] Moreover, MMT clay is a very soft phyllosilicate group of minerals, which is effective as an adsorptive of heavy metals as well as toxic substance, and also can be used as a medicine to treat contact dermatitis for external use.[34,35] Despite these encouraging deductions, related toxicological studies are yet to be conducted and the actual risks inherent to the use of nanoparticles remain difficult to ascertain. Therefore, it is recommended to work in a well-ventilated room or in the direction of the wind, and wear adequate personal protective equipment.

Conclusions

In summary, it takes only more than ten minutes to prepare the novel AuNCs@MMT nanocomposites with red fluorescence, which is attributed to the superheating, non-thermal effects and high pressure induced by microwave irradiation and electrostatic adsorption between BSA–Au NCs bioconjugates and MMT clay powders. Layered structure of MMT clay provides enough surfaces for loading Au NCs, which increased the fluorescent emission of AuNCs@MMT nanocomposites and decreased the aggregation of Au NCs powders. The processing is environment-friendly and the products are user-friendly. The as-prepared fluorescent powders were successfully applied to latent fingerprints visualizations by powdering technique. As a result, strong contrasts as well as clear and distinguishable ridge details were obtained with the facile operation. Satisfactory patterns and

ridges with a bright red fluorescence were presented under UV light (365 nm). Furthermore, green light (510 nm) can be applied to excite the AuNCs@MMT nanocomposites to avoid common background fluorescence interferences and UV damage for examiners. As such, it should be attractive for applications in surfaces with and complex patterns and colours. In addition, this nontoxic powder without any organic solvent and dyes can reduce the harm for the operators. Hence, due to its unique photoluminescence property, good sensitivity, no toxicity, strong resistance to background interference and user-friendly operation, the as-prepared AuNCs@MMT nano-composites powder is an actual alternative to conventional powdering reagents.

Conflicts of interest

There are no conflicts to declare.

Acknowledgements

Notes and references

1 C. Xu, R. Zhou, W. He, L. Wu, P. Wu and X. Hou, *Anal. Chem.*, 2014, **86**, 3279–3283.

2 Y. Li, C. Xu, C. Shu, X. Hou and P. Wu, *Chin. Chem. Lett.*, 2017, DOI: 10.1016/j.cclet.2017.04.027.

3 P. Wu, C. Xu, X. Hou, J. J. Xu and H. Y. Chen, *Chem. Sci.*, 2015, **6**, 4445–4450.

4 J. Dilag, H. Kobus, Y. Yu, C. T. Gibson and A. V. Ellis, *Polym. Int.*, 2015, **64**, 884–891.

5 J. Chen, J. S. Wei, P. Zhang, X. Q. Niu, W. Zhao, Z. Y. Zhu, H. Ding and H. M. Xiong, *ACS Appl. Mater. Interfaces*, 2017, **9**, 18429–18433.

6 M. Saif, *J. Lumin.*, 2013, **135**, 187–195.

7 M. J. Choi, A. M. McDonagh, P. J. Maynard and C. Roux, *Forensic Sci. Int.*, 2008, **179**, 87–97.

8 X. Yu, J. Liu, S. Zuo, Y. Yu, K. Cai and R. Yang, *Forensic Sci. Int.*, 2013, **231**, 125–130.

9 P. Niu, B. Liu, Y. Li, Q. Wang, A. Dong and H. Hou, *Dyes Pigm.*, 2015, **119**, 1–11.

10 G. P. Darshan, H. B. Premkumar, H. Nagabhushana, S. C. Sharma, S. C. Prashanth and B. D. Prasad, *J. Colloid Interface Sci.*, 2016, **464**, 206–218.

11 G. Saunders, *74th Annual Edueational Conference*. Pensaeola, USA, 1989.

12 B. Schnetz and P. Margot, *Forensic Sci. Int.*, 2001, **118**, 21–28.

13 M. J. Choi, K. E. McBean and R. Wuhrer, *Journal of Forensic Identification*, 2006, **56**, 24–32.

14 E. Stauffer, A. Becue and K. V. Singh, *Forensic Sci. Int.*, 2007, **168**, e5–e9.

15 D. Gao, F. Li and J. Song, *Talanta*, 2009, **80**, 479–483.

16 R. Leggett, E. E. Lee-Smith and S. M. Jickells, *Angew. Chem., Int. Ed.*, 2007, **46**, 4100–4103.

17 T. Peng, W. Qin, K. Wang, J. Shi, C. Fan and D. Li, *Anal. Chem.*, 2015, **87**, 9403–9407.

18 K. Li, W. Qin, F. Li, X. Zhao, B. Jiang, K. Wang, S. Deng, C. Fan and D. Li, *Angew. Chem., Int. Ed.*, 2013, **52**, 11542–11545.

19 I. Hussain, S. Z. Hussain and R. Habib ur, *Nanoscale*, 2010, **2**, 2575–2578.

20 G. Qin, M. Zhang and Y. Zhang, *J. Electroanal. Chem.*, 2013, **693**, 122–126.

21 F. Gao, C. Lv, J. Han, X. Li, Q. Wang, J. Zhang, C. Chen, Q. Li, X. Sun, J. Zheng, L. Bao and X. Li, *J. Phys. Chem. C*, 2011, **115**, 21574–21583.

22 L. Yan, Y. Cai, B. Zheng, Y. Guo and D. Xiao, *J. Mater. Chem.*, 2012, **22**, 1000–1005.

23 X. Yang, M. Shi, R. Zhou, X. Chen and H. Chen, *Nanoscale*, 2011, **3**, 2596–2601.

24 J. Zheng, J. T. Petty and R. M. Dickson, *J. Am. Chem. Soc.*, 2003, **125**, 7780.

25 Y. Bao, C. Zhong, D. M. Vu, J. P. Temirov, R. B. Dyer and J. S. Martinez, *J. Phys. Chem. C*, 2007, **111**, 12194.

26 H. W. Duan and S. M. Nie, *J. Am. Chem. Soc.*, 2007, **129**, 2412.

27 Y. Negishi, K. Nobusada and T. Tsukuda, *J. Am. Chem. Soc.*, 2005, **127**, 5261.

28 J. P. Xie, Y. G. Zheng and J. Y. Ying, *J. Am. Chem. Soc.*, 2009, **131**, 888–889.

29 P. A. Buffat, M. Fl€ueli and R. Spycher, *Faraday Discuss.*, 1991, **92**, 173–187.

30 G. S. Sodhi and J. Kaur, *Forensic Sci. Int.*, 2001, **120**, 172–176.

31 H. Li, H. Huang and A. Wang, *Sens. Actuators, B*, 2017, **241**, 1057–1062.

32 H. Li, J. Chen and H. Huang, *Sens. Actuators, B*, 2016, **223**, 40–44.

33 H. Chen, B. Li and X. Ren, *Biomaterials*, 2012, **33**, 8461–8476.

34 K. G. Bhattacharyya and S. S. Gupta, *Adv. Colloid Interface Sci.*, 2008, **140**, 114–131.

35 J. Saary, R. Qureshi and V. Palda, *J. Am. Acad. Dermatol.*, 2005, **53**, 845e1–845e13.